文章编号:1006-9941(2023)07-0688-11

UHPLC-QTOF-MS High Efficiency Eetectionof Impurities in a Typical CL-20 Synthesis Process

SU Peng-fei[1,2], **E Xiu-tian-feng**[1], **Ma Ting-ting**[1], **HU Yin**[1,2], **WANG Min-chang**[1,2], **ZHANG Gao**[2], **MENG Zi-hui**[2,3]

(1. *College of Chemistry and Chemical Engineering, Beijing Institute of Technology, Beijing* 100081, *China*; 2. *Xi'an Modern Chemistry Research Institute, Xi'an* 710065, *China*; 3. *Yangtze Delta Region Academy of Beijing Institute of Technology, Jiaxing* 314003, *China*)

Abstract: Quickly and accurately detect and analyze the intermediates and impurities produced in the synthesis of Hexanitrohexaazaisowurtzitane (CL-20), is important for controlling the purity or quality of CL-20, and ensuring its sensitivity and detonation performance. In this study, nuclear magnetic resonance (NMR) and ultra-high performance liquid chromatography-Quadrupole time-of-flight mass spectrometry (UHPLC-QTOF-MS) were used to rapidly and efficiently analyze the impurities in the typical synthesis process of CL-20. The results showed that the impurity in HBIW was 1,3-dibenzyl imidazole, the impurity in tetraacetyl dibenzyl hexazepane (TADB) was low acylated triacetyl tribenzyl hexazepane (TATB), and the impurity in tetraacetyl hexazepane (TAIW) was incomplete TADB. The impurities in CL-20 were not fully nitrated monoacetyl pentanitrohexazazine (MPIW) and diacetyl tetranitrohexazazine (DATN).

Key words: CL-20; intermediates; impurities; UHPLC-QTOF-MS; NMR

CLC number: TJ55; O65 **Document code**: A **DOI**: 10.11943/CJEM2023070

0 Introduction

High energy density materials (HEDM) are widely used in military fields such as explosives, propellants, pyrotechnics and fireworks, and can rapidly release a large amount of stored chemical energy when actuated. 2,4,6,8,10,12-hexanitro-2,4,6,8,10,12-hexaazaisowurtzitane (CL-20 or HNIW) is one of the most powerful explosives with a high nitrogen content (six N—NO_2 groups) and a tight polycyclic-cage structure[1]. It is expected to replace commercially used hexahydro-1, 3, 5-trinitro-1, 3, 5-triazine (RDX) and 1, 3, 5, 7-tetranitro-1, 3, 5, 7-tetraazecycloctane (HMX) (which has 14%−20% more energy than HMX)[2−6]. A considerable amount of research for optimizing the synthesis pathway, process conditions, and crystallization method of CL-20 has been reported[7−13]. Nevertheless, the high mechanical sensitivity and easy phase transition of CL-20 have hindered its practical applications. Therefore, many approaches offer great potential to produce less sensitive energetic CL-20-based materials, such as promoting crystal quality[14−15], coating the crystal surface with insensitive explosives[16], and cocrystallizing with other compounds[17]. But these methods also obviously reduce detonation performances of CL-20.

Actually, the impurities contained in CL-20 could also affect its mechanical sensitivity, seriously damaging its safety and long-term stability. Accurate detection and analysis of intermediates' purity and type during the CL-20 synthesis process, and further

Received Date: 2023-04-04; **Revised Date**: 2023-05-25

Published Online: 2023-06-28

Grant support: National Natural Science Foundation of China (22105024)

Bipgraphy: SU Peng-fei (1978−), male, master degree, mainly engaged in explosive analysis and detection technology research. e-mail: 95601943@qq.com

Corresponding author: E Xiu-tian-feng (1990−), female, associate researcher/doctor degree, mainly engaged in the synthesis and analysis of aerospace propellants and energetic materials.
e-mail: xtf_e@bit.edu.cn

引用本文:苏鹏飞,鄂秀天凤,马婷婷,等. UHPLC-QTOF-MS高效检测CL-20合成过程的杂质[J]. 含能材料,2023,31(7):688−698.
SU Peng-fei, E Xiu-tian-feng, Ma Ting-ting,et al. UHPLC-QTOF-MS High Efficiency Eetectionof Impurities in a Typical CL-20 Synthesis Process[J]. *Chinese Journal of Energetic Materials (Hanneng Cailiao)*, 2023, 31(7):688−698.

purification will be a choice to improve the quality of CL-20 without reducing its detonation performance. At present, most researches focus on the analysis of morphology or purity of the final products by GC-MS, HPLC, NMR, Raman, or FTIR, and so on[18-24]. However, the intermediates and impurities produced during the synthesis process have a certain impact on the quality of the final CL-20, and there is no systematic detection and analysis. Therefore, the of impurities in the synthesis of CL-20 is urgently needed.

Accordingly, we developed a method to identify the endogenous impurities in the synthesis process by ultra-high performance liquid chromatography-quadrupole time of flight mass spectrometry (UPLC-QTOF-MS) analysis. It has both HPLC analysis method of high efficient separation ability, but also has high sensitivity of mass spectrometry and detection ability[25]. In this work, CL-20 and its intermediates were prepared by typical synthesis routes. The main intermediates and final product of each step in the synthesis of CL-20 were preliminarily determined by the commonly used NMR measurements. Then, an UHPLC-QTOF-MS analysis was conducted to qualitatively determine the product composition of each intermediate and final product. This work would provide technical support for CL-20 quality control.

1 Materials and Methods

1.1 Materials

Benzylamine (98%) and glyoxal (99%) were purchased from Aladdin. Fuming nitric acid (AR grade, 95%) and acetonitrile (LC-MS grade, 99.9%) were obtained from J&K Chemical. Formic acid (LC-MS grade, 99.9%) was obtained from Sigma-Aldrich. Pd/C was purchased from Shaanxi Rock New Materials Co. Ltd. All chemicals were used directly without further purification. The deionized water was obtained in the lab and the ultrapure water was produced by a Milli-Q water system (Millipore, MA, USA).

1.2 Synthesis process of CL-20

CL-20 and its intermediates were synthesized in the laboratory of Beijing Institute of Technology, adopting the most commonly used methods (Scheme 1), i.e. 2,4,6,8,10,12-hexabenzyl-2,4,6,8,10,12-hexaazaisowurtzitane (HBIW) was first formed by the condensation of three glyoxal molecules with six benzylamine molecules in acetonitrile using a protic acid (formic acid) as a catalyst. HBIW is then hydrolyzed to obtain2,6,8,12-tetraacetyl-4,10-dibenzyl-2,4,6,8,10,12-hexaazaisowurtzitane (TADB)[26]. Using the one-pot process, TADB can be directly nitrated to CL-20 with a yield of 82%[27]. Besides, the secondary catalytic hydrogenolysis of TADB in acetic acid will produce 2,6,8,12-tetraacetyl-2,4,6,8,10,12-hexaazaisowurtzitane(TAIW)[28], and then TAIW nitrification to CL-20 with a yield of 95%[29]. The purity of the compounds determined by high performance liquid chromatography were above 98% .

1.3 NMR analysis

The structure of CL-20 and its intermediates was analyzed by ^{1}H NMR and ^{13}C NMR spectrum using a Bruker Avance 500M Spectrometer equipped with a

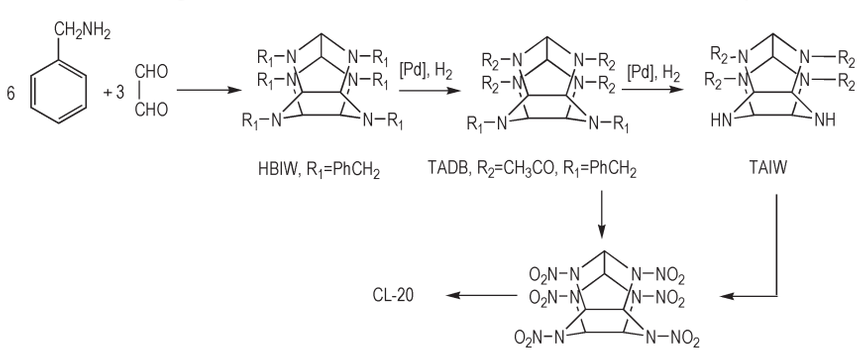

Scheme 1 Synthesis route of CL-20

5 mm inverse probe and operated at 500.16 MHz and 298 K. The operating software was Bruker's Topspin software version 3.2 (Bruker Biospin, Germany). Before being injected into a nuclear magnetic sample tube, the CL-20 sample was dissolved in DMSO, and the three main intermediate samples were dissolved in $CDCl_3$ using tetramethylsilane (TMS) as the internal standard. The nuclear magnetic sample tube was tightly sealed before the NMR test.

1.4 UHPLC-QTOF-MS analysis

Before the UHPLC-QTOF-MS analysis, 10 mg dried and finely powdered samples (CL-20, HBIW, TAIW) were dissolved in 1 mg·mL^{-1} acetonitrile, and 10 mg dried TADB sample was dissolved in 1 mg·mL^{-1} acetic acid. Then, diluting the above samples to a concentration of 10 μg·mL^{-1} using acetonitrile, and sealed storing the samples in small bottles waiting for the test.

The UHPLC analysis was conducted using an ACQUITY™ UP LC system with an ACQUITY UPLC HSS C_{18} column (50 mm×2.1 mm, 1.8 μm, USA Waters company). The mobile phase consisted of solvent A (0.1% formic acid aqueous solution) and solvent B (100% acetonitrile). The flow rate of mobile phase was 0.25 mL·min^{-1} using a gradient elution program shown in Table 1. Each injection volume was 5 μL, and the column temperature was set at 30 ℃. The mass detection was carried out using a SYNAPT™ HDMS equipped with a Z-spray electrospray interface (USA Waters company), and the ion source was electrospray ionization (ESI). The operating software was MassLynx software version 4.1 (Waters, Milford, MA), and the optimized operating conditions for electrospray ionization mass spectrometry (ESI-MS) were listed in Table 2. By adjusting the wavelength scanning range, it was found that CL-20, TADB, TAIW and HBIW only had impurity peaks at their maximum UV absorption. So, the detection wavelength of CL-20, TADB, TAIW, HBIW were selected as 225, 205, 205 nm and 204 nm, respectively.

Table 1 The gradient elution program of UHPLC in this test

time / min	flow rate / mL·min^{-1}	A / %, v/v	B / %, v/v
0	0.25	85	15
2	0.25	50	50
8	0.25	5	95
9	0.25	50	50
10	0.25	85	15

Note: A is 0.1% formic acid aqueous solution, and B is 100% acetonitrile.

Table 2 Operating conditions of ESI-MS in this test

parameter	ESI-MS	
resolution	9000	
mode	full scan/dd MS^2	
mass range / Da	100 to 1000	
polarity	positive	negative
capillary voltage / kV	3	2
cone / V	35	35
source temperature / ℃	100	100
desolvation temperature / ℃	300	300
cone gas flow / L·h^{-1}	50	50
desolvation gas flow / L·h^{-1}	300	300

2 Results and discussion

2.1 NMR analysis of CL-20 and its intermediates

The main product structure at each step of the CL-20 synthesis process was determined by NMR spectrum. Fig.1 and Fig.2 show the ^{1}H NMR and ^{13}C NMR spectra of the three main intermediates (Intermediate Ⅰ, Ⅱ and Ⅲ) and the final product. Twelve absorption peak groups in ^{13}C NMR spectra of Intermediate I indicate that there are twelve types of carbon atoms in different chemical environments in the molecular structure (Fig.1a). According to calculated values of chemical shift, peak shape and coupling constant, the signals at δ=141.0−140.0 represent the quaternary carbon on the aromatic ring, the signals at δ=130.0−126.0 represent carbon on the aromatic ring, the signals at δ=81.0−76.0 represent carbon on the isowurtzitane, and the signals at δ=58.0−55.0 represent carbon on the benzyl. Fig.1b shows the ^{1}H NMR spectra of Intermediate Ⅰ, and there are 48 protons with an integral ratio (from high to low field) of about 2∶4∶9∶4∶30. Combined with the previous discussion, the signals at δ=7.50−7.00

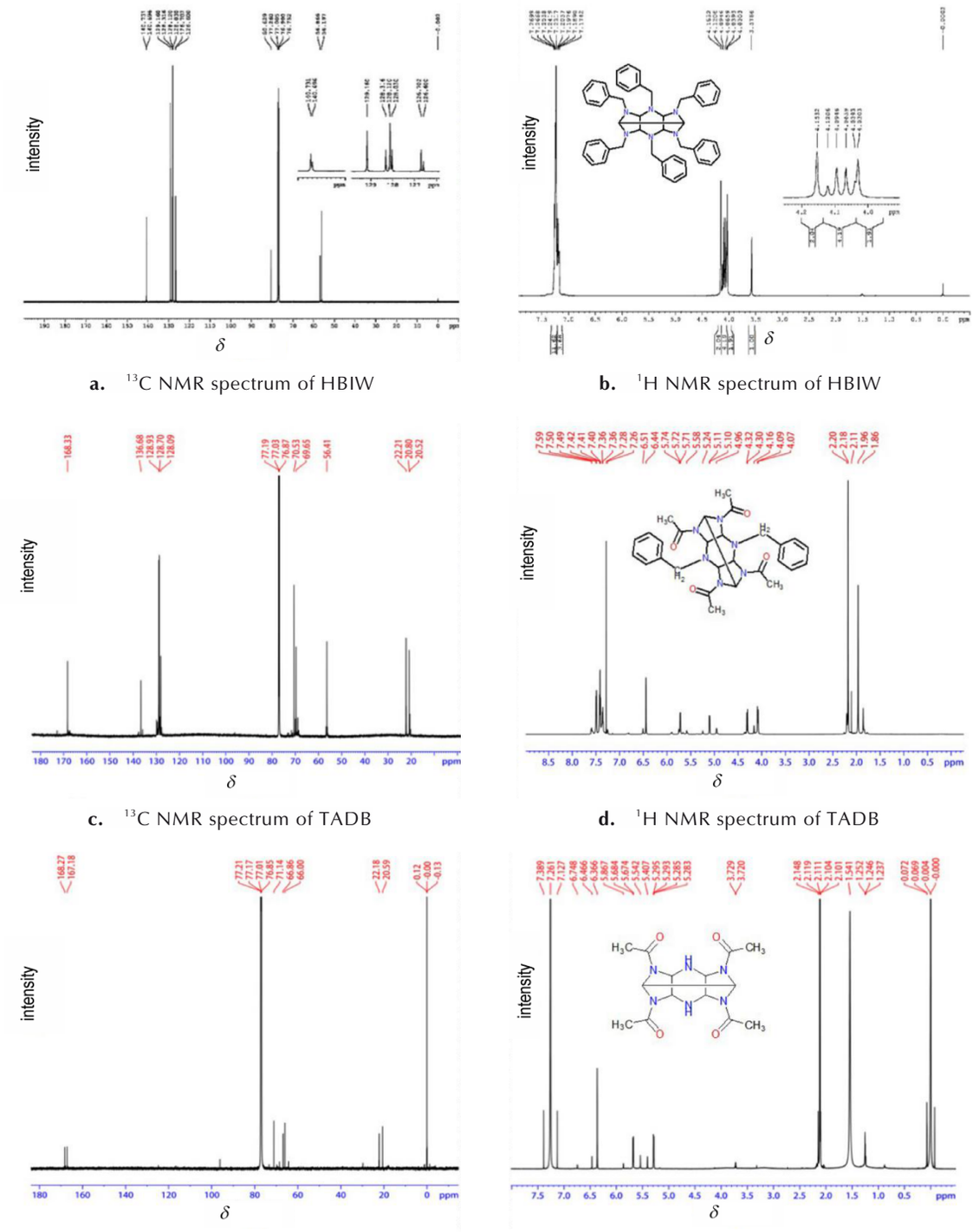

a. ^{13}C NMR spectrum of HBIW **b.** ^{1}H NMR spectrum of HBIW

c. ^{13}C NMR spectrum of TADB **d.** ^{1}H NMR spectrum of TADB

e. ^{13}C NMR spectrum of TAIW **f.** ^{1}H NMR spectrum of TAIW

Fig.1 ^{13}C NMR and ^{1}H NMR spectrum of the three intermediates

(m, 30H) represent six single substitution hydrogen on the aromatic rings, the signals at δ=4.15 (s, 4H) represent hydrogen on the hexatomic ring, the signals at δ=4.13−3.90 (m, 12H) represent hydrogen on the submethyl of the benzyl group which give multiple peaks due to the molecular asymmetry, and the signals at δ=3.58 (s, 2H) represent hydrogen on the bridge structure of isowurtzitane. So it can be concluded that Intermediate Ⅰ is HBIW. Fig.1c and 1d show that there are 10 types of carbon atoms and 32 protons with an integral ratio (from high to low field) of ca. 12∶4∶4∶2∶10 in the molecu-

lar structure of Intermediate Ⅱ. Fig.1e and 1f show that there are 7 types of carbon atoms and 20 protons with an integral ratio (from high to low field) of ca. 12∶2∶4∶2 in the molecular structure of Intermediate Ⅲ. Types of hydrogen and carbon represented by each signal are summarized in the Table 3 and Table 4. It can be seen that Intermediate Ⅱ and Ⅲ are identified as TADB and TAIW, respectively.

At the same time, the final product was also confirmed by NMR analysis. As shown in Fig. 2a, there are two absorption peak groups in ^{13}C NMR spectra indicating two types of carbon atoms in different chemical environments in the molecular structure. The signals at δ=75.1 represent carbons on the hexagonal ring skeleton of isowurtzitane, and the signals at δ=72.2 represent carbons on the pentagon ring skeleton of isowurtzitane. Fig.2b shows 6 protons with an integral ratio (from high to low field) of ca. 2∶1 in the molecular structure. As the analysis method mentioned above, the signals at δ=8.21 (s, 2H) represent hydrogen on the pentagon ring skeleton of isowurtzitane, and the signals at δ=8.35 (s, 4H) represent hydrogen on

Table 3 Carbon types to each signal in three intermediates and CL-20

compound	δ value	carbon types
HBIW	141.0−140.0	quaternary C on the aromatic ring
	130.0−126.0	C on the aromatic ring
	81.0−76.0	C on the isowurtzitane
	58.0−55.0	C on the benzyl
TADB	175.0−168.0	carbonyl C on acetyl group
	140.0−135.0	quaternary C on the aromatic ring
	130.0−128.0	C on the aromatic ring
	75.0−65.0	C on the isowurtzitane
	60.0−54.0	C on the benzyl
	24.0−18.0	C on the acetyl methyl
TAIW	169.0−167.0	carbonyl C on the acetyl group
	75.0−62.0	C on the pentagon ring skeleton of isowurtzitane
	25.0−7.0	C on the acetyl methyl
CL-20	75.1	C on the hexagonal ring skeleton of isowurtzitane
	72.2	C on the pentagon ring skeleton of isowurtzitane

Table 4 Hydrogen types to each signal in three intermediates and CL-20

compound	δ value	hydrogen types
HBIW	7.50−7.00	six single substitution H on the aromatic rings
	4.15	H on the hexatomic ring
	4.13−3.90	H on the submethyl of the benzyl group
	3.58	H on the bridge structure of isowurtzitane
TADB	7.80−7.00	H on the aromatic ring
	7.00−6.20	H on the bridge structure of isowurtzitane
	6.10−4.60	H on the hexagonal ring skeleton of isowurtzitane
	4.50−3.70	H on the benzyl
	2.40−1.60	H on the acetyl methyl
TAIW	6.80−6.10	H connecting with carbon atoms of isowurtzitane
	6.00−5.10	H connecting with carbon atoms of isowurtzitane
	4.30−2.80	H connecting with nitrogen atoms of isowurtzitane
	2.30−1.80	H on the acetyl methyl
CL-20	8.21	H on the pentagon ring skeleton of isowurtzitane
	8.35	H on the hexagonal ring skeleton of isowurtzitane

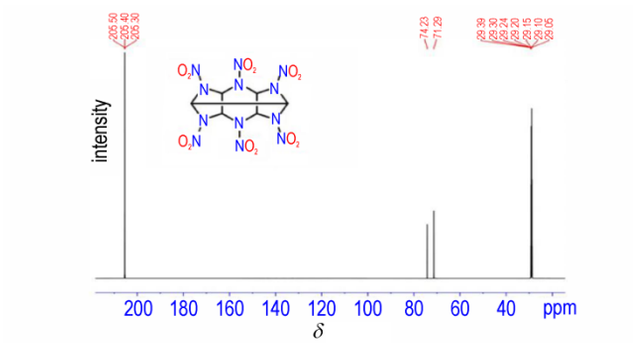

a. ^{13}C-NMR spectrum

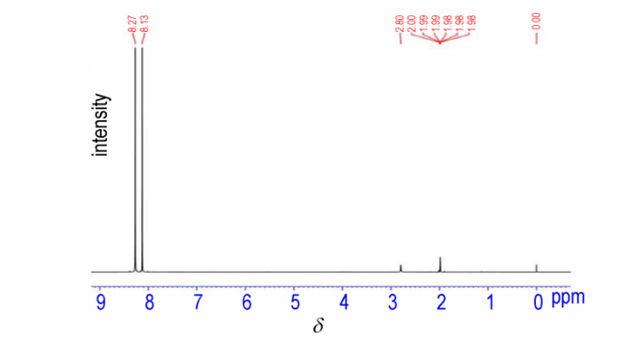

b. ^{1}H-NMR spectrum

Fig.2 NMR spectrum of CL-20

the hexagonal ring skeleton of isowurtzitane. These results confirm that the final product is CL-20.

2.2 UHPLC-QTOF-MS analysis of impurities

UHPLC-QTOF-MS has high efficiency separation ability, high sensitivity and detection ability which can qualitatively determine the product components of each step in the CL-20 synthesis process. In this work, the three intermediates namely HBIW, TADB and TAIW were scanned in a positive ion mode, and CL-20 was scanned in a negative ion mode. The liquid phase chromatography of each product composition was basically the same as their total ion current diagram, so the liquid phase chromatography and ESI-MS results of each product composition will be detailedly discussed in the following.

2.2.1 Impurities in HBIW

Fig.3 shows the liquid phase chromatography of HBIW and its main impurity at the resident time of 1.26 min and 1.14 min, respectively. According to the ESI-MS of HBIW in Fig.4a, the positive ion mode of HBIW is [M+H]$^+$ at m/z=709.3924, and there are two complementary ion pairs at m/z=237.1356

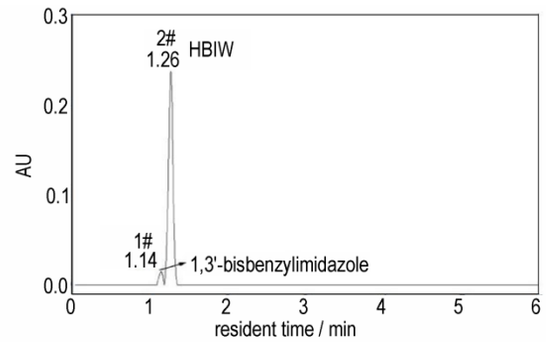

Fig.3 Liquid phase chromatography of HBIW and its main impurity

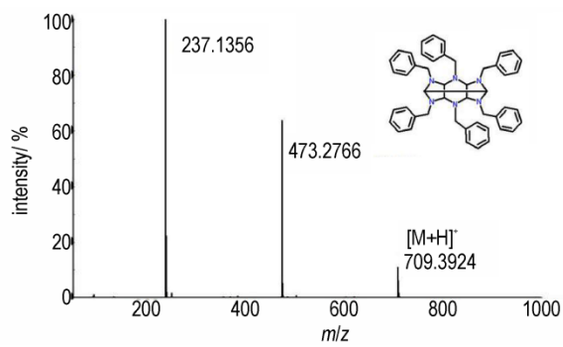

a. HBIW

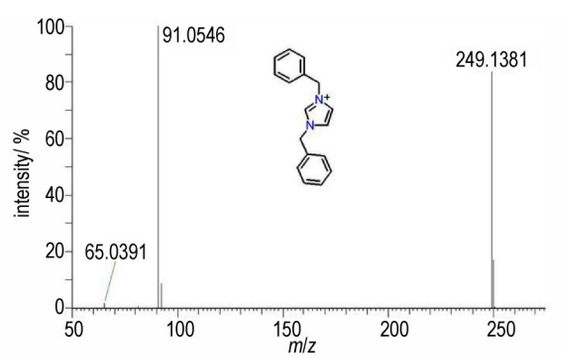

b. 1,3-dibenzylimidazole

Fig.4 Positive ESI-MS and ESI-MS^2 spectrum

and m/z=473.2766 after the ring cracking in the ESI-MS^2 spectrum. Then, an elemental fitting is conducted due to the ESI-MS result of the main impurity in Fig. 4b, suggesting the molecular formula is $C_{17}H_{17}N_2$, and its unsaturation degree is calculated of 10.5. Further, the ESI-MS^2 spectrum data at m/z= 91.0546 indicates there is a benzyl group in the molecular structure, indicating the impurity is 1, 3-dibenzylimidazole.

2.2.2 Impurities in TADB

Fig.5 shows the liquid phase chromatography of TADB and its main impurity at the resident time of

4.74 min and 4.88 min, respectively. According to the ESI-MS of TADB in Fig.6a, the positive ion mode of TADB is $[M+H]^+$ at m/z=517.2648, and the main fragmentation pathway is consistent with its structural features in the ESI-MS^2 spectrum (Fig.6b). The positive ion mode of the main impurity is $[M+H]^+$ at m/z=565.2839 (Fig.7a), and the molecular formula is suggested as $C_{33}H_{36}N_6O_3$ by elemental fitting, which adds C_5H_4 and reduces one oxygen atom compared to TADB ($C_{28}H_{32}N_6O_4$), indicating an acetyl group leaving the TADB and adding a benzyl group in the structure. Combined with the fragmentation

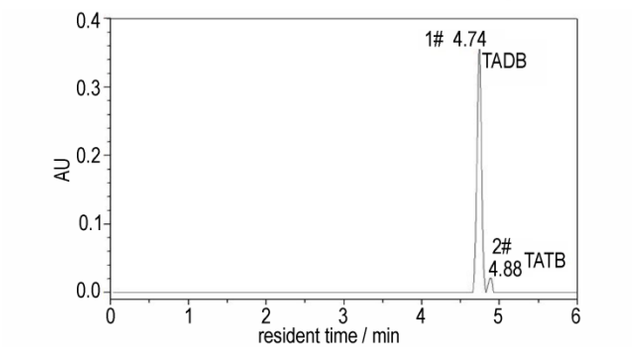

Fig. 5 Liquid phase chromatography of TADB and its main impurity

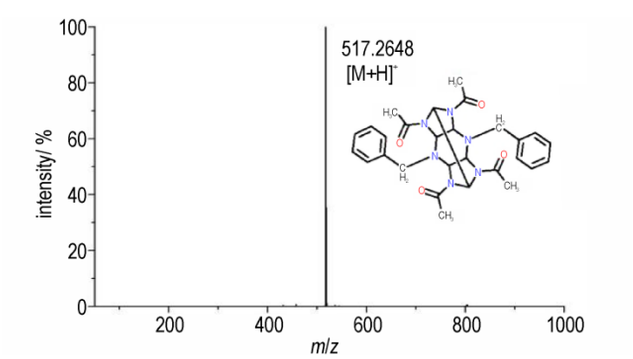

a. ESI-MS spectrum

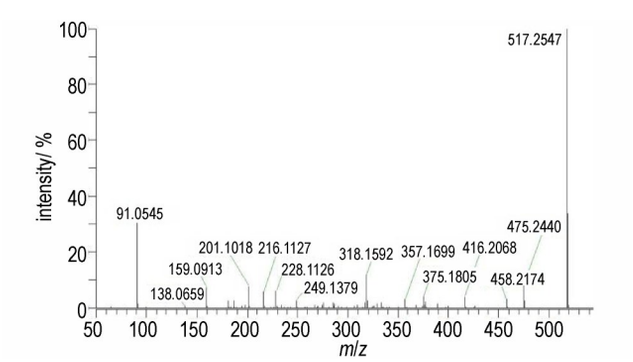

b. ESI-MS^2 spectrum

Fig.6 Positive ESI-MS and ESI-MS^2 spectrum of TADB

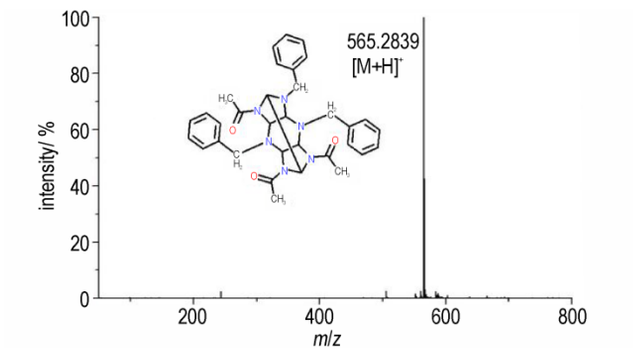

a. ESI-MS spectrum

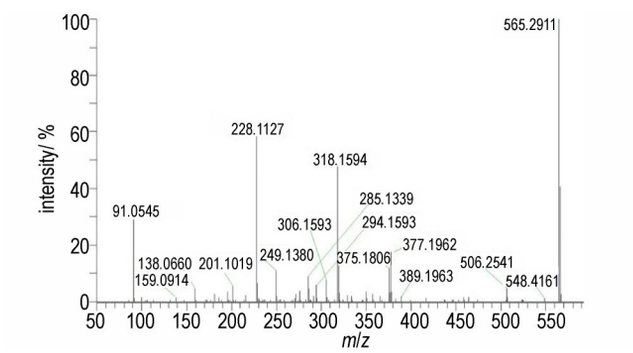

b. ESI-MS^2 spectrum

Fig.7 Positive ESI-MS and ESI-MS^2 spectrum of TATB

pathway in the ESI-MS^2 spectrum (Fig.7b), the impurity in TADB is triacetyltribenzylhexaazaisowurtzitane (TATB).

2.2.3 Impurities in TAIW

Fig.8 shows the liquid phase chromatography of TAIW and its main impurity at the resident time of 1.62 min and 4.74 min, respectively. According to the ESI-MS spectrum in Fig. 9a, the positive ion mode of TAIW is $[M+H]^+$ at m/z=337.1614, and the main fragmentation pathway is consistent with its structural features in the ESI-MS^2 spectrum (Fig.9b). The positive ion mode of the main impurity is $[M+H]^+$ at m/z=517.2648 (Fig. 6a), and the molecular formula is suggested as $C_{28}H_{32}N_6O_4$ by elemental fitting, which adds $C_{14}H_{12}$ compared to TAIW ($C_{14}H_{20}N_6O_4$), indicating two benzyl groups were added to the TAIW structure. The main fragmentation pathways shown in Fig. 6b are fragment ion at m/z=475.2440 by hydrogen rearrangement deethylketone (CH_2CO), m/z=458.2174 by ring cracking deethylamide, m/z=416.2068 by further deethylketone, and m/z=357.1699 by ring opening

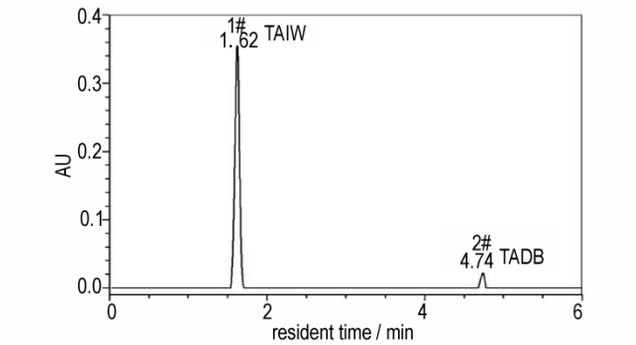

Fig.8 Liquid phase chromatography of TAIW and its main impurity

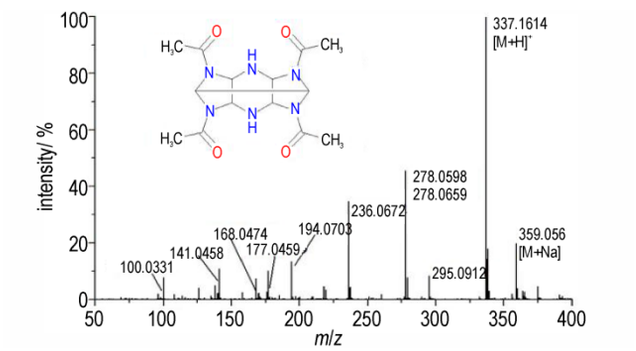

a. ESI-MS spectrum

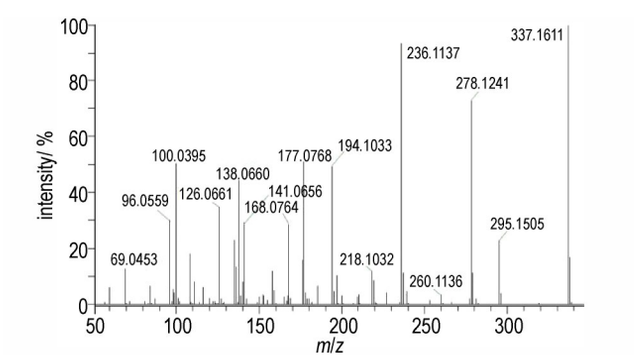

b. ESI-MS^2 spectrum

Fig.9 Positive ESI-MS and ESI-MS^2 spectrum of TAIW

deethylamide. The characteristic ion at m/z= 91.0545 with a low mass end is benzyl group. Thus, the main impurity in TAIW is identified as TADB.

2.2.4 Impurities in CL-20

The liquid chromatograph in Fig.10 shows that, there are two main impurities in CL-20 (3.06 min) with a resident time of 2.38 min (Impurity Ⅰ) and 2.54 min (Impurity Ⅱ), respectively. The nitro groups in the CL-20 usually have a strong electron absorption, which makes CL-20 not ionized in the positive ion mode, but ionized well in the negative ion mode in ESI-MS test. Fig.11a shows that CL-20

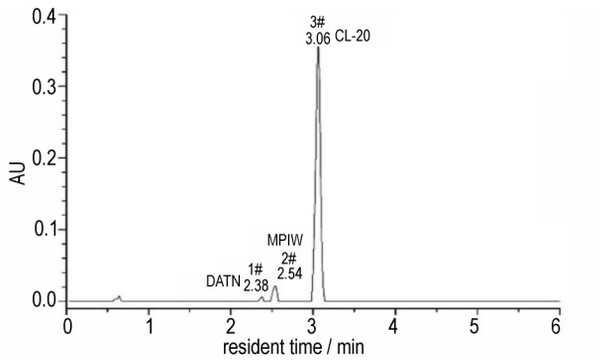

Fig.10 Liquid phase chromatography of CL-20 and its main impurities

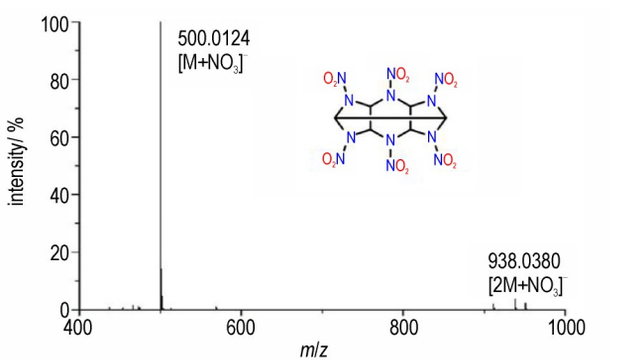

a. CL-20

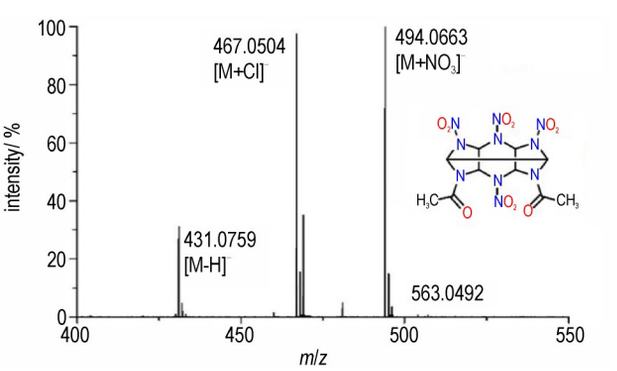

b. DATN

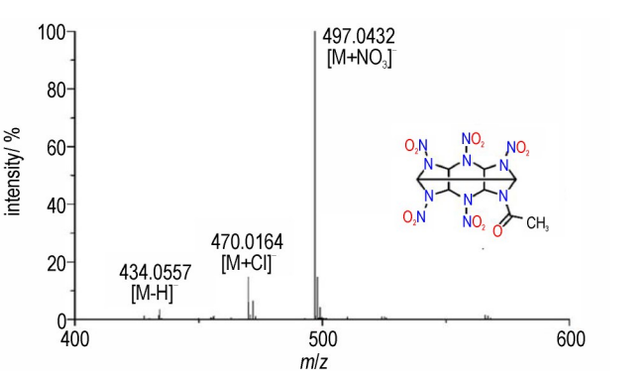

c. MPIW

Fig.11 Negative ESI-MS spectrum of CL-20 and its impurities

gives two negative ions which are $[M+NO_3]^-$ at m/z=500.0124 and $[2M+NO_3]^-$ at m/z=938.0380. There are three negative ion modes of Impurity Ⅰ in Fig.11b, i.e. $[M+NO_3]^-$ at m/z=494.0663, $[M+Cl]^-$ at m/z=467.0504, and a weak $[M-H]^-$ ion at m/z=431.0759. The molecular formula of Impurity Ⅰ is suggested as $C_{10}H_{12}N_{10}O_{10}$ by elemental fitting, which adds C_4H_6 and reduces N_2O_2 compared to CL-20 ($C_6H_6N_{12}O_{12}$), indicating two acetyl groups were added and two nitro groups were removed from the CL-20 structure. Impurity Ⅱ also has three negative ion modes which are $[M+NO_3]^-$ at m/z=497.0432, $[M+Cl]^-$ at m/z=470.0164 and $[M-H]^-$ at m/z=434.0557 (Fig.11c). Its molecular formula is fitted to $C_8H_9N_{11}O_{11}$. Compared to CL-20, C_2H_3 is added and NO is reduced, indicating that an acetyl group is added to the structure of CL-20 and a nitro group is removed. Because the ionization type is additive ions, only NO_3^- (m/z=61.9870) without other ion fragments was obtained in the ESI-MS^2 of CL-20 and its two impurities. Therefore, combined with the reaction pathway and mechanism, it can be concluded that Impurity Ⅰ is diaceryltetranitrohexaazaisowurtzitane (DATN), and Impurity Ⅱ is unnitrated monoacetylpentanitrohexaazaisowurtzitane (MPIW).

So far, the main product and its impurities in each step of CL-20 synthesis process were confirmed by NMR and UHPLC-QTOF-MS analysis, and the results were summarized in Table 5.

Table 5 Product components identified by UHPLC-QTOF-MS

number	resident time / min	selected ion	molecular formula	MS^2 / Da	theoretical M_w / Da	detected M_w / error, mDa	product components
1	1.14	$[M+H]^+$	$C_{17}H_{17}N_2$	91.0546	249.1386	249.1378(−0.8)	1,3-dibenzylimidazole
	1.26	$[M+H]^+$	$C_{48}H_{48}N_6$	473.2766 237.1356	709.4019	709.3924(9.5)	HIBW
2	4.74	$[M+H]^+$	$C_{28}H_{32}N_6O_4$	−	517.2563	517.2648(0.9)	TADB
	4.88	$[M+H]^+$	$C_{33}H_{36}N_6O_3$	−	565.2927	565.2839(1.6)	TATB
3	1.62	$[M+H]^+$	$C_{14}H_{20}N_6O_4$	−	337.1624	337.1614(1.0)	TAIW
	4.74	$[M+H]^+$	$C_{28}H_{32}N_6O_4$	−	517.2563	517.2648(0.9)	TADB
4	2.38	$[M+NO_3]^-$	$C_{10}H_{12}N_{10}O_{10}$	61.9870	494.0616	494.0663(−4.7)	DATN
	2.54	$[M+NO_3]^-$	$C_8H_9N_{11}O_{11}$	61.9870	497.0361	497.0432(−7.1)	MPIW
	3.06	$[M+NO_3]^-$	$C_6H_6N_{12}O_{12}$	61.9870	500.0106	500.0124(−1.8)	CL-20

Note: M_w is the monoisotopic mass.

3 Conclusions

We developed a simple strategy to improve the quality of CL-20 in an attempt to ensure its detonation performance by accurately and quickly detecting and analyzing impurities in the synthesis of CL-20. The main conclusions are as follows:

(1) The intermediates HBIW, TADB, TAIW and the product CL-20 were identified by ^{13}C-NMR and ^{1}H-NMR.

(2) The UPLC-QTOF-MS analysis showed that the impurities in HBIW were mainly 1, 3-dibenzylimidazole, the impurity in TADB was TATB, the impurity in TAIW was the unreacted TADB in the previous step, and the impurities in CL-20 were MPIW and DATN.

References:

[1] NIELSEN A T, CHAFIN A P, CHRISTIAN S L, et al. Synthesis of polyazapolycyclic caged polynitramines [J]. *Tetrahedron*, 1998, 54(39): 11793−11812.

[2] HANG G Y, YU W L, TAO W, et al. Theoretical investigations on stabilities, sensitivity, energetic performance and mechanical properties of CL-20/NTO cocrystal explosives by molecular dynamics simulation [J]. *Theoretical Chemistry Accounts*, 2018, 137(8): 11401−11414.

[3] SIDER A K, SIKDER N, GANDHE B R, et al. Hexanitrohexaazaisowurtzitane or CL-20 in India: Synthesis and characterization [J]. *Defence Science Journal*, 2012, 52 (2):

135-146.

[4] AGRAWAL J. Some new high energy materials and their formulations for specialized applications[J]. *Propellants Explosives Pyrotechnics*, 2010, 30(5): 316-328.

[5] TALAWAR M B, SIVABALAN R, ASTHANA S N, et al. Novel ultrahigh-energy materials[J]. *Combustion Explosion & Shock Waves*, 2005, 41(3): 264-277.

[6] LI Y, SONG J, LI C, et al. Theoretical predictions on the structures and properties for several novel hexaazaisowurtzitane derivatives-Looking for HEDC[J]. *Acta Chimica Sinica*, 2009, 67(13): 1437-1446.

[7] JIN S, SHU Q, CHEN S. Preparation of epsilon-HNIW by a one-pot method in concentrated nitric acid from tetraacetyldiformylhexaazaisowurtzitane [J]. *Propellants Explosives Pyrotechnics*, 2007, 32(6): 468-471.

[8] QIAN H, YE ZW, LV CX. An efficient and facile synthesis of hexanitrohexaazaisowurtzitane (HNIW)[J]. *Letters in Organic Chemistry*, 2007, 4(7): 482-485.

[9] BAYAT Y, MOKHTARI J. Preparation of 2, 4, 6, 8, 10, 12-hexanitro-2,4,6,8,10,12-hexaazaisowurtzitane from 2,6,8,12-tetraacetyl 2,4,6,8,12-hexaazaisowurtzitane using various nitrating agents[J]. *Defence Science Journal*, 2011, 61(2): 171-173.

[10] BAYAT Y, HAJIGHASEMALI F. An efficient and facile synthesis of CL-20 from TADNO using HNO_3/N_2O_5 and optimization of reaction parameters by Taguchi method[J]. *Propellants Explosives Pyrotechnics*, 2016, 41(5): 893-898.

[11] SIVAKUMAR D, VEMBU S, CHANDRAKUMARI S, et al. One-pot synthesis of hexaacetylhexaazaisowurtzitane (HAIW) a precursor of 2, 4, 6, 8, 10, 12-hexanitro-2, 4, 6, 8, 10, 12-hexaazaisowurtzitane (HNIW-CL20) [J]. *Chemistry Select*, 2017, 2(10): 3014-3017.

[12] NIELSEN AT, CHAFIN AP, CHRISTIAN SL, et al. Synthesis of polyazapolycyclic caged polynitramines [J]. *Tetrahedron*, 1998, 54(39): 11793-11812.

[13] ANTOINE EDM VAN DER HEIJDEN, RICHARD HB BOUMA. Crystallization and characterization of RDX, HMX, and CL-20 [J]. *Crystal Growth & Design*, 2004, 4(5): 999-1007.

[14] SHANG Y, JIN B, PENG R, et al. A novel 3D energetic MOF of high energy content: Synthesis and superior explosive performance of a Pb(ii) compound with 5,5′-bistetrazole-1,1′-diolate[J]. *Dalton Transactions: An International Journal of Inorganic Chemistry*, 2016, 45 (35): 13881-13887.

[15] SUN C, ZHANG C, JIANG C, et al. Synthesis of AgN_5 and its extended 3D energetic framework [J]. *Nature Communications*, 2018(9): 1269-1273.

[16] KIM KJ, KIM HS. Coating of energetic materials using crystallization[J]. *Chemical Engineering Technology*, 2010, 28(8): 946-951.

[17] AN C, LI H, YE B, et al. Nano-CL-20/HMX cocrystal explosive for significantly reduced mechanical sensitivity[J]. *Journal of Nanomaterials*, https://doi.org/10.1155/2017/3791320.

[18] JIE L J, SHI R B. Application of high performance liquid chromatography in experiment teaching[J]. *Research and Exploration in Laboratory*, 2010, 29 (2): 14-15.

[19] PERSSON B, ÖSTMARK H, BERGMAN H. An HPLC method for analysis of HNIW and TNAZ in an explosive mixture[J]. *Propellants Explosives Pyrotechnics*, 2010, 22(4): 238-239.

[20] MAKAROV A, LOBRUTTO R, CHRISTODOULATOS C, et al. The use of ultra high-performance liquid chromatography for studying hydrolysis kinetics of CL-20 and related energetic compounds[J]. *Journal of Hazardous Materials*, 2009, 162 (2-3): 1034-1040.

[21] GOEDE P, LATYPOV N, STMARK H. Fourier transform raman spectroscopy of the four crystallographic phases of α,β,γ and ε 2,4,6,8,10,12-hexanitro-2,4,6,8,10,12- hexaazatetracyclo[5.5.0.0(5,9).0(3,11)]dodecane (HNIW, CL-20)[J]. *Propellants Explosives Pyrotechnics*, 2004, 29(4): 205-208.

[22] XUAN H, YU L, HUANG S, et al. Raman spectroscopy coupled with principal component analysis to quantitatively analyze four crystallographic phases of explosive CL-20[J]. *RSC Advances*, 2018, 8(41): 23348-23352.

[23] KHOLOD Y, OKOVYTYY S, KURAMSHINA G, et al. An analysis of stable forms of CL-20: A DFT study of conformational transitions, infrared and Raman spectra[J]. *Journal of Molecular Structure*, 2007, 843(1-3): 14-25.

[24] PAN Q, SU PF, GAO HX, et al. Quantitative determination of CL-20 polymorphs by mid-infrared diffuse reflectance spectroscopy[J]. *Chinese Journal of Energetic Materials*(*Hanneng Cailiao*), 2016, 24(5): 503-508.

[25] SISCO E, STAYMATES M E, FORBES T P. Optimization of confined direct analysis in real time mass spectrometry (DART-MS)[J]. *Analyst*, 2020, 145(7): 2743-2750.

[26] LATYPOV NV, WELLMAR U, GOEDE P, et al. Synthesis and scale-up of 2, 4, 6, 8, 10, 12-hexanitro-2, 4, 6, 8, 10, 12-hexaazaisowurtzitane from 2, 6, 8, 12-tetraacetyl-4, 10-dibenzyl-2, 4, 6, 8, 10, 12-hexaazaisowurtzitane (HNIW, CL-20)[J]. *Organic Process Research & Development*, 2014, 4(3): 156-158.

[27] WANG C, OU Y, CHEN B. One-pot synthesis of hexanitrohexaazaisowurtzitane[J]. *Journal of Beijing Institute of Technology*, 2000 (4): 521-523.

[28] DONG K, SU C H, SONG J W, et al. Synthesis of 2, 6, 8, 12-tetraacetyl-2, 4, 6, 8, 10, 12-hexaazaisowurtzitane (TAIW) from 2, 6, 8, 12-tetraacetyl-4, 10-dibenzyl-2, 4, 6, 8, 10, 12-hexaazaisowurtzitane (TADBIW) by catalytic hydrogenolysis using a continuous flow process[J]. *Organic Process Research & Development*, 2014, 18(11): 1321-1325.

[29] ZHAO X, MA P. A novel method for preparing HNIW with concentrated nitric acid[J]. *Acta Armamentarii*, 2002 (01): 27-29.

UHPLC-QTOF-MS高效检测CL-20合成过程的杂质

苏鹏飞[1,2],鄂秀天凤[1],马婷婷[1],胡 银[1,2],王民昌[1,2],张 皋[2],孟子晖[2,3]
(1. 北京理工大学化学与化工学院,北京 100081;2. 西安近代化学研究所,西安 710065;3. 北京理工大学长三角研究院,嘉兴 314003)

摘 要: 为了快速准确检测和分析六硝基六氮杂异伍兹烷(CL-20)合成过程中产生的中间体和杂质,控制CL-20纯度或品质,保证其感度及爆轰性能,采用核磁共振(NMR)和超高高效液相色谱-四极杆飞行时间质谱(UHPLC-QTOF-MS)技术快速、高效分析检测了CL-20典型合成工艺过程中组分及杂质。结果表明,六苄基六氮杂异伍兹烷(HBIW)中的杂质为1,3-二苄基咪唑,四乙酰基二苄基六氮杂异伍兹烷(TADB)中的杂质为低酰基化的三乙酰基三苄基六氮杂异伍兹烷(TATB),四乙酰基六氮杂异伍兹烷(TAIW)中的杂质为未完全反应的TADB,CL-20中的杂质为未完全硝化的一乙酰基五硝基六氮杂异伍兹烷(MPIW)和二乙酰基四硝基六氮杂异伍兹烷(DATN)。

关键词: CL-20;中间体;杂质;UHPLC-QTOF-MS;NMR
中图分类号: TJ55;O65 **文献标志码:** A **DOI:** 10.11943/CJEM2023070
基金项目: 国家自然科学基金资助(22105024)

(责编:高 毅)